# Suppression of Anoikis by *SKP2* Amplification and Overexpression Promotes Metastasis of Esophageal Squamous Cell Carcinoma

**Xiao-Chun Wang,[1] Yu-Peng Wu,[1] Bo Ye,[2] De-Chen Lin,[1] Yan-Bin Feng,[1] Zi-Qiang Zhang,[3] Xin Xu,[1] Ya-Ling Han,[1] Yan Cai,[1] Jin-Tang Dong,[4] Qi-Min Zhan,[1] Min Wu,[1] and Ming-Rong Wang[1]**

*[1]State Key Laboratory of Molecular Oncology, [2]Department of Thoracic Surgery, and [3]Central Laboratory, Cancer Institute (Hospital), Peking Union Medical College and Chinese Academy of Medical Sciences, Beijing, China; and [4]Winship Cancer Institute, Emory University School of Medicine, Atlanta, Georgia*

## Abstract

**The gene of SKP2, located on chromosome 5p13, plays a critical role in cell cycle progression, especially at the $G_1$-S transition, putatively through its control of several cell cycle regulator proteins including $p27^{kip1}$, $p21^{cip1}$, $p57^{kip2}$, p130, cyclin E, and c-Myc. Previous studies in this laboratory revealed that gain of chromosome 5p was often seen in esophageal squamous cell carcinoma (ESCC). In the present study, we examined the amplification status and expression level of SKP2 in ESCC and investigated its clinicopathologic significance. Amplification and elevated expression of SKP2 correlated significantly with tumor stage and positive lymph node metastasis ($P < 0.05$). The SKP2 protein expression level as determined by immunohistochemical staining showed a significant inverse correlation with p27 protein. *In vivo* assay showed that inhibition of SKP2 expression also decreased tumor growth and lung metastasis of ESCC cells. At the molecular level, knockdown of SKP2 by RNA interference inhibited cell migration and invasion ability. Knockdown of SKP2 expression sensitized cancer cells to anoikis, and a wobble mutant of SKP2 that is resistant to SKP2 small interfering RNA can rescue this effect. Expression level of pAkt decreased after SKP2 knockdown. Treatment of cells with phosphoinositidyl 3-kinase inhibitor (LY294002) and constitutively activator (insulin-like growth factor I) had significant effects on the anoikis of SKP2 RNA interference cells. These results show for the first time that SKP2 is amplified and overexpressed in ESCC. Elevated expression of SKP2 protected cancer cells from anoikis, and this effect was mediated, at least in part, by the phosphoinositidyl 3-kinase-Akt pathway. (Mol Cancer Res 2009;7(1):12–22)**

## Introduction

Esophageal squamous cell carcinoma (ESCC) is one of the most common malignant tumors in China, but little is known about the major oncogenes involved in the tumorigenesis of this disease. Accumulated evidence suggests that multiple genetic alterations occurring sequentially in a cell lineage, at both nucleotide level and chromosome level, underlie the carcinogenetic process in solid tumors. Amplification of chromosomal DNA is one of the mechanisms capable of activating genes whose overexpression contributes to development and progression of cancer. Several studies, including our report, have shown that gain in DNA copy number within the short arm of chromosome 5 (5p) occurred frequently in ESCC, non–small-cell lung cancers, and oral squamous cell carcinomas (1-4), suggesting that chromosome 5p may harbor some target genes whose amplification rendered them oncogenic in these tumors.

SKP2 was discovered by Zhang et al. in 1995 (5) and mapped on chromosome 5p13 (6). It is a member of the F-box family and constitutes the substrate recognition subunit of the $SCF^{SKP2}$ ubiquitin ligase complex. The most important substrates for SKP2 include $p27^{kip1}$ cyclin-dependent kinase inhibitor and cyclin E, both of which interact with cyclin-dependent kinase 2 to regulate $G_1$-S transition (7). SKP2 has also been implicated in regulating the proteosome-mediated degradation of c-myc, $p21^{cip1}$, $p57^{kip2}$, and p130-Rb2 (8-13). Elevated SKP2 expression has been shown in breast, colorectum, lung, and stomach carcinomas and lymphomas (14-16). Fukuchi et al. (17) reported that expression levels of SKP2 and p27 were negatively correlated in early ESCC. Overexpression of SKP2 has been found to correlate with lymph node metastasis in several kinds of tumors, but the potential mechanisms are still unknown. We here reported amplification and overexpression of SKP2 in ESCC. Statistical analysis revealed that both amplification and overexpression of SKP2 correlated with lymph node metastasis and tumor stage. Significantly inverse correlation between SKP2 and p27

Received 2/15/08; revised 9/30/08; accepted 10/6/08.
**Grant support:** National Science Fund grants 30630067 and 30721001, State Key Basic Research Grant of China no. 2004CB518705, National Key Technologies R&D Program of China grant 2006BAI02A14, and Chinese Hi-Tech R&D Program Grant no. 2006AA02A403.
The costs of publication of this article were defrayed in part by the payment of page charges. This article must therefore be hereby marked *advertisement* in accordance with 18 U.S.C. Section 1734 solely to indicate this fact.
**Note:** Supplementary data for this article are available at Molecular Cancer Research Online (http://mcr.aacrjournals.org/).
**Requests for reprints:** Ming-Rong Wang, State Key Laboratory of Molecular Oncology, Cancer Institute (Hospital), Peking Union Medical College and Chinese Academy of Medical Sciences, P.O. Box 2258, Beijing 100021, China. Phone: 86-10-87788425; Fax: 86-10-87778651. E-mail: wangmr04@126.com

doi:10.1158/1541-7786.MCR-08-0092

expression was found in ESCC. Cellular function experiments showed that decreased expression of SKP2 by RNA interference (RNAi) impaired the migration and invasion capacity of esophageal cancer cells. In addition, our data indicated that SKP2 promotes anoikis resistance through the phosphoinositidyl 3-kinase (PI3K)-Akt pathway.

## Results

### *Amplification and Overexpression of SKP2 in ESCC*

Our earlier comparative genomic hybridization studies had shown high-level gains of chromosome 5p in ESCC tissues. Therefore, we determined copy numbers of *SKP2* by fluorescence *in situ* hybridization (FISH) in ESCC. Amplification of *SKP2* gene was observed in 23 of 50 (46%) tumors. Signals of 5q35 probe (RP11-51d11) as control indicated that the increase in *SKP2* copy number did not result from polyploidy of chromosome 5 (Fig. 1A). We did not find any case showing chromosome 5 polyploidy in the present series. Positive correlation was found between *SKP2* amplification, tumor stage, and lymph node metastases ($P < 0.05$; Table 1). To confirm this result, real-time PCR was done in 10 cases (tumors and matched adjacent histologic normal epithelia). Glyceraldehyde-3-phosphate dehydrogenase (*GAPDH*) was applied as the internal reference (Fig. 1B). Melting curves were done to confirm the PCR specificity (Supplementary Fig. S1). Increased DNA dosage was observed in 5 of 10 (50%) tumors (data not shown).

We next examined the SKP2 mRNA expression by reverse transcription-PCR in eight esophageal carcinomas that had shown amplification in FISH examination. Elevated SKP2 mRNA level was observed in six tumors as compared with the adjacent normal epithelia (Fig. 1C). Western blotting displayed

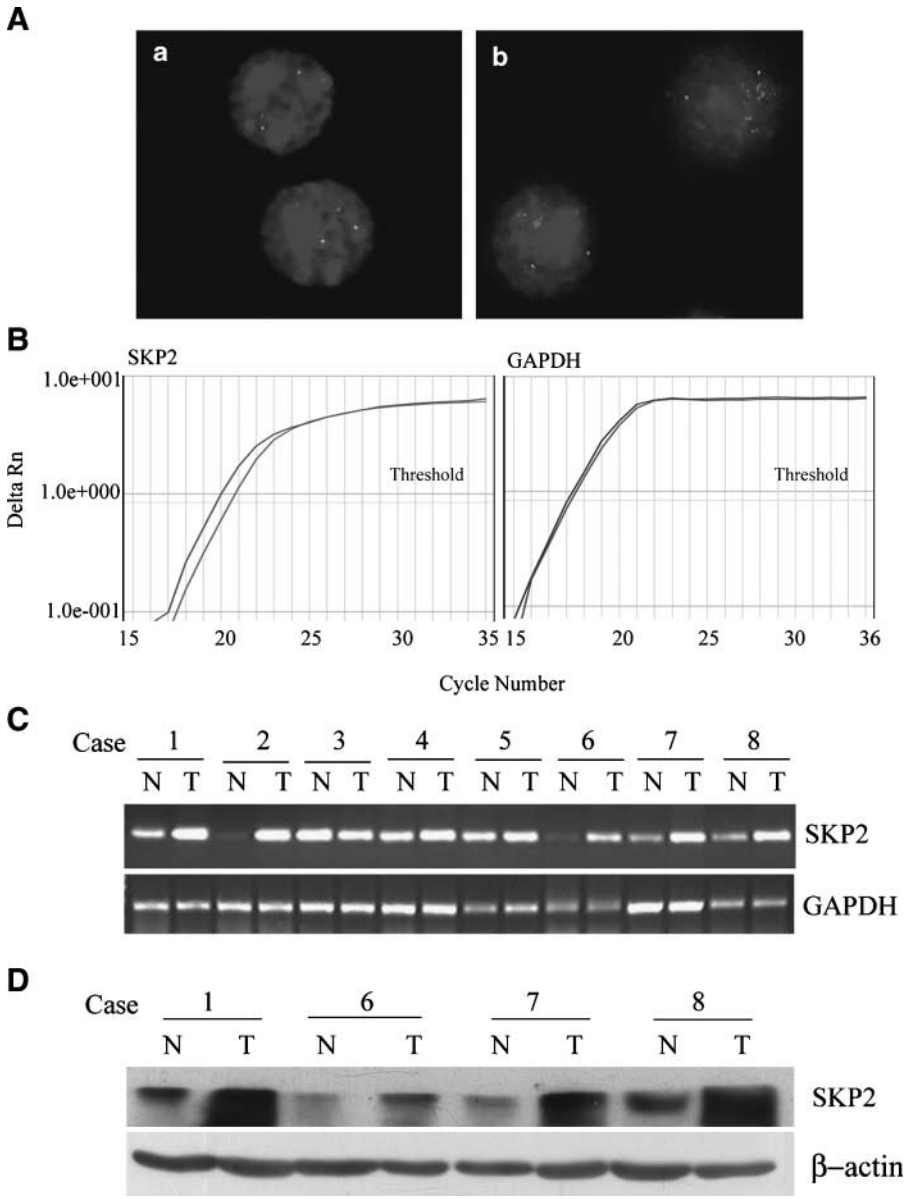


**FIGURE 1.** Amplification and overexpression of SKP2 in ESCC. **A.** Representative images of two-color FISH for *SKP2*. **a**, the BAC of RP11-816N21 (containing *SKP2* gene; *red*) and RP11-51d11 (control; *green*) generated two signals in normal peripheral blood lymphocytes. **b**, esophageal squamous carcinoma cells contain multiple or cluster signals of SKP2 but only two copies of the control probe. **B.** Real-time PCR detection of SKP2 and GAPDH in matched esophageal tumors and normal epithelia. SKP2 copy number was higher in the tumor than in the normal epithelial tissue compared with GAPDH as control. **C.** Up-regulated SKP2 mRNA level was detected in six of eight tumors (*T*) as compared with normal adjacent epithelia (*N*) by reverse transcription-PCR. **D.** Western blotting shows that SKP2 protein level was increased in malignant tissues.

**Table 1. Relationship between SKP2 Amplification and Overexpression with Tumor Clinicopathologic Features**

| Clinicopathologic Features | SKP2 Amplification | | | | SKP2 Expression | | | | |
|---|---|---|---|---|---|---|---|---|---|
| | *n* | No Amplification, *n* (%) | Amplification,* *n* (%) | *P* | *n* | Negative* *n* (%) | Positive,* *n* (%) | Strongly positive,* *n* (%) | *P* |
| TNM classification | | | | | | | | | |
| pT | | | | | | | | | |
| $pT_1 + pT_2$ | 10 | 7 (14) | 3 (6) | 0.308 † | 17 | 12 (8.6) | 3 (2.1) | 2 (1.4) | 0.121 † |
| $pT_3 + pT_4$ | 40 | 20 (40) | 20 (40) | | 123 | 56 (40) | 28 (20) | 39 (27.9) | |
| Lymph node metastasis | | | | | | | | | |
| $N_0$ | 26 | 20 (40) | 6 (12) | 0.007 † | 68 | 38 (27.1) | 17 (12.1) | 13 (9.3) | 0.037 † |
| $N_1$ | 24 | 7 (14) | 17 (34) | | 72 | 30 (21.4) | 14 (10) | 28 (20) | |
| Stage | | | | | | | | | |
| I + II | 28 | 21 (42) | 7 (14) | 0.001 † | 74 | 43 (30.7) | 17 (12.1) | 14 (10) | 0.013 † |
| III + IV | 22 | 6 (12) | 16 (32) | | 66 | 25 (17.9) | 14 (10) | 27 (19.3) | |
| Grade | | | | | | | | | |
| 1 | 27 | 16 (32) | 11 (22) | 0.309 ‡ | 60 | 32 (22.9) | 12 (8.6) | 16 (11.4) | 0.431 ‡ |
| 2 | 16 | 8 (16) | 8 (16) | | 59 | 27 (19.3) | 17 (12.1) | 15 (10.7) | |
| 3 | 7 | 3 (6) | 4 (8) | | 21 | 9 (6.4) | 2 (1.4) | 10 (7.1) | |

*For definition, see text.
† Kruskal-Wallis test.
‡ Mann-Whitney test.

that SKP2 protein increased in all of the four examined malignant tissues (Fig. 1D).

To clarify the potential relationship between elevated expression of SKP2 and various clinicopathologic parameters, immunohistochemical analysis was done on the tissue microarray using anti-SKP2 antibody. In normal epithelia, most cells showed no or weak SKP2 expression. In contrast to the normal epithelia, high expression of SKP2 was observed in 72 of 140 (51%) ESCC (Fig. 2A). Statistical analysis indicated that elevated expression of SKP2 was significantly associated with tumor stage and positive lymph node metastasis ($P < 0.05$; Table 1). Given that $p27^{kip1}$ was one of the mainly substrates of $SCF^{SKP2}$ ubiquitin ligase complex, we also measured p27 expression in these tissues by immunohistochemistry (Fig. 2B). Significant negative correlation was found between SKP2 and $p27^{kip1}$ expression (Supplementary Fig. S2; Supplementary Table S1). To explore whether SKP2 level is just a surrogate marker for cell cycling, expression of Ki67 as a proliferation control was also examined (Fig. 2C). No correlation was found between SKP2 and Ki67 expression (Supplementary Table S1).

### *Decreased Expression of SKP2 in EC9706 Cells Inhibits Invasion and Migration*

Because elevated expression of SKP2 correlated with lymph node metastasis, we examined whether excess SKP2 is involved in invasiveness. Reduction of SKP2 protein inhibited the ability of cells to invade surrounding tissues, as determined by Matrigel assay (Fig. 3B). We also examined cell migration because it is an important component of the invasive process. EC9706 cells treated with SKP2 RNAi showed decreased ability to migrate through membranes of 8-μm pore size that were not coated with Matrigel (Fig. 3B). These experiments had been repeated thrice and the results were similar. We also examined the expression of p27 and p21 after SKP2 knockdown in EC9706 cells using Western blotting. Expression levels of p27 and p21 increased in SKP2 RNAi cells (Fig. 3A).

### *Knockdown of SKP2 Promoted Anoikis of EC9706 Cells*

Given that SKP2 overexpression correlated with lymphoid metastasis and anoikis is one type of apoptosis involved in tumor metastasis (18), we tested the detachment-induced apoptosis. As shown in Fig. 4A, total percent (early and late apoptosis) of apoptotic SKP2 RNAi cells was about double that of the control and parental cells in the assessment by Annexin V-FITC/propidium iodide staining. Repeated experiment data are shown in Fig. 4B.

We then examined the effects of SKP2 knockdown on cell cycle progress, p27 and p21 expression, and caspase-3 activity (a central mediator of apoptosis) in the context of anchorage

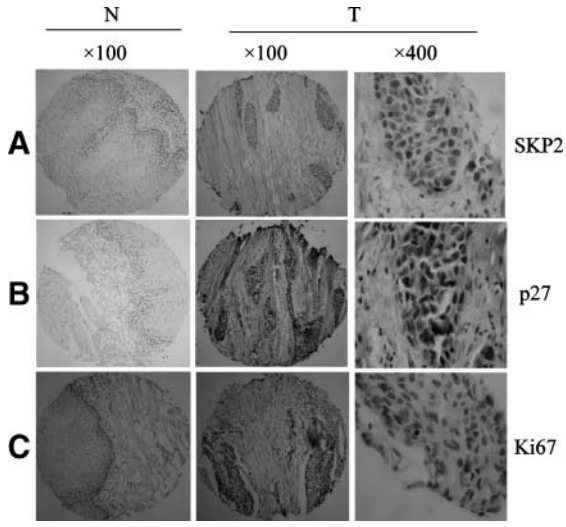


**FIGURE 2.** Representative SKP2, p27, and Ki67 immunostaining in an esophageal carcinoma and normal epithelia of the same case. **A.** Low expression of SKP2 was detected in normal esophageal epithelium. Esophageal squamous carcinoma cells were strongly stained. **B.** High expression of p27 was detected in normal esophageal epithelium, but p27 was negative in esophageal squamous carcinoma cells. **C.** Low expression of Ki67 was detected in normal esophageal epithelium and stained negatively in esophageal squamous carcinoma cells.

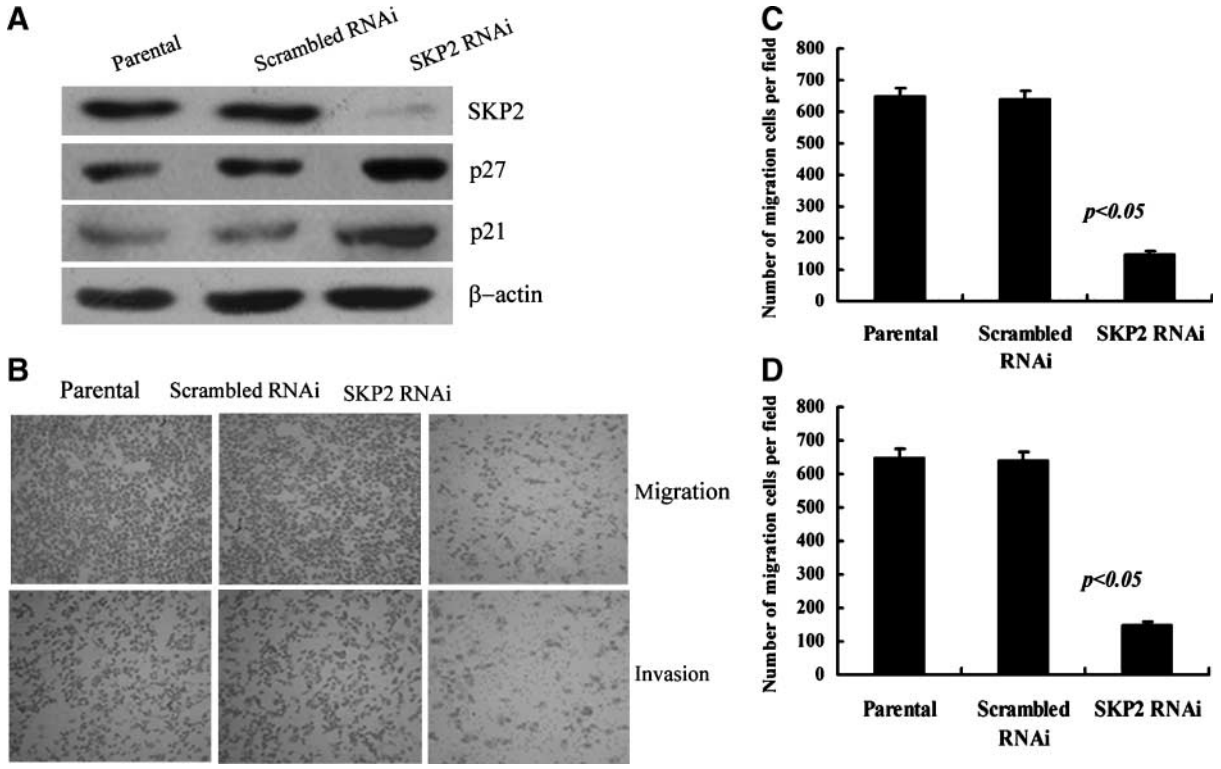


**FIGURE 3.** Inhibition of cell migration and invasion by RNAi mediated reduction of SKP2 expression. **A.** Western blotting analysis of SKP2 expression in stably transfected SKP2 RNAi, scrambled RNAi, and parental EC9706 cells. SKP2 RNAi exhibited down-regulation of SKP2 and up-regulation of p27 and p21. **B.** Representative photos of haptotactic migration assay and Matrigel chemoinvasion assay in SKP2 RNAi, scrambled RNAi, and parental EC9706 cells. **C** and **D.** Statistical plots of migration and Matrigel chemoinvasion assay. The number of SKP2 RNAi cells transversed in the transwell membranes in haptotactic migration assay and Matrigel chemoinvasion assay was significantly decreased compared with the scrambled and parental EC9706 cells. Columns, mean of three independent experiments; bars, SD.

deprivation. During induction of anoikis on polyHEMA plates, decreased SKP2 expression markedly increased expression of p27 and p21 protein and activity of caspase-3 compared with parental or scrambled RNAi controls (Fig. 4C). However, no significant difference in cell cycle progress was found between these three groups (Fig. 4D and E).

To verify that the effects of RNAi described above are specific, we prepared a SKP2 construct bearing triple-point mutation in the 19-bp sequence that served as target for short hairpin RNA (shRNA)–mediated knockdown in our experiments. The mutation conserved the amino acid sequence of the SKP2 protein but rendered its expression insensitive to inhibition by the shRNA. Transfection of this mutant shRNA into the cells with stable expression of SKP2-shRNA, indeed, restored the ability of SKP2 to inhibit anoikis (Fig. 5A and B). Next, we detected the effect of p27 on anoikis. As shown in Fig. 5C and D, knockdown of p27 had no effect on both attached and detached EC9706 cells.

### *Silencing of SKP2 in EC9706 Promoted Anoikis via Inactivation of the PI3K-Akt Pathway*

We subsequently examined the potential effect of SKP2 on the activation of several known pathways associated with anoikis to explore the molecular mechanism by which SKP2 protected EC9706 cells from anoikis. The activation of PI3K-Akt, mitogen-activated protein kinase/extracellular signal–regulated kinase (Erk) kinase (MEK)-Erk, and epidermal growth factor receptor (EGFR) signaling was measured by Akt phosphorylation on Ser473, Erk phosphorylation on Tyr204, and EGFR expression, respectively, after transfection with SKP2 small interfering RNA (siRNA) in EC9706 cells. Only phosphorylated Akt was down-regulated in SKP2 siRNA cells. No changes in Erk activation or EGFR expression were observed in these three groups of cells (Fig. 6C), suggesting that they were not downstream targets accounting for the protective effect against anoikis of SKP2. We next treated the cells cultured on polyHEMA-coated dishes with the PI3K inhibitor LY294002 and constitutive activator insulin-like growth factor I, respectively. As shown in Fig. 6A and B, the percentages of anoikis cells in SKP2 RNAi group after adding LY294002 or insulin-like growth factor I were not significantly different from those of control groups, suggesting that the PI3K-Akt pathway is the downstream target of SKP2 and that SKP2 can protect EC9706 cells from anoikis via this pathway.

### *Reduced SKP2 Expression in EC9706 Inhibited Colony Formation in Soft Agar and Subcutaneous Tumor Growth in Nude Mice*

Given that anchorage-independent growth is a characteristic of malignantly transformed cells, we performed the colony

formation assay in soft agar. Colony-forming activity of SKP2 RNAi cells under anchorage-independent condition was markedly decreased as compared with scrambled RNAi and parental EC9706 cells (Fig. 7A). Subsequently, subcutaneous tumor growth assays in nude mice were done to examine the effect of SKP2 on tumor growth *in vivo*. SKP2 RNAi, scrambled RNAi, and parental EC9706 cells were inoculated subcutaneously into nude mice. Tumors were observed in all three groups, but the tumors formed by scrambled RNAi or parental EC9706 cells grew faster than in SKP2 RNAi–treated mice. At 12 weeks postinfection, the mice were sacrificed. Tumor weights of scrambled RNAi or parental EC9706 cells were significantly heavier than those of the tumors formed by SKP2 RNAi ($P < 0.05$; Fig. 7B). In addition, two mice inoculated

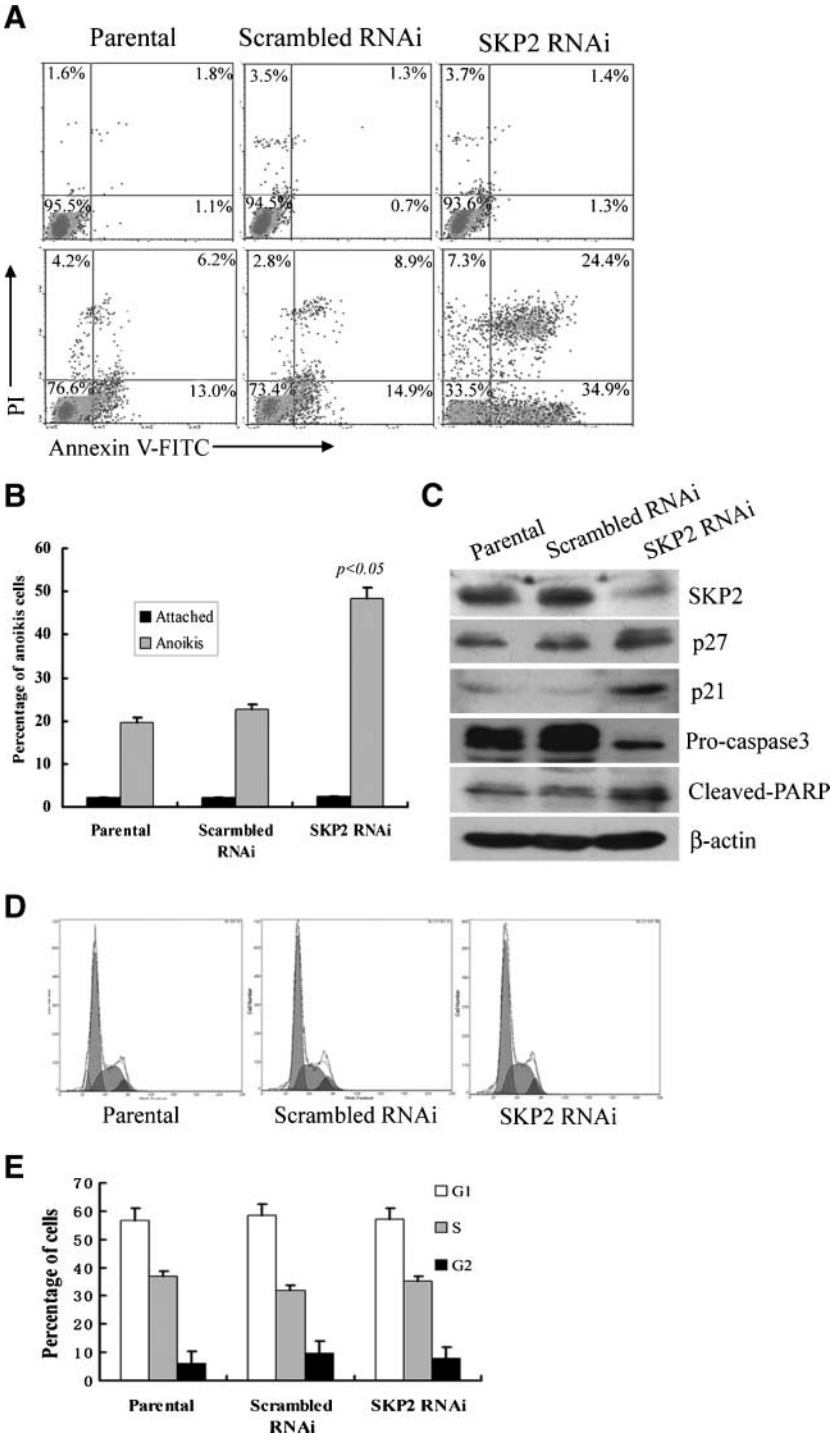


**FIGURE 4.** Effects of SKP2 knockdown on anoikis and cell cycle progress in detached EC9706 cells. **A.** Representative images of flow cytometry analysis of apoptotic cells by Annexin V-FITC/propidium iodide staining. **B.** Flow cytometry results were plotted as mean from triplicate experiments; bars, SD. $P < 0.05$, versus scrambled RNAi or parental EC9706 cells. **C.** Reduced expression of SKP2 led to increased p27 and p21 expression and promoted caspase-mediated anoikis in EC9706 cells. **D.** Representative images of flow cytometry analysis of cell cycle by propidium iodide staining. **E.** Flow cytometry results of cell cycle were plotted as mean from triplicate experiments; bars, SD.

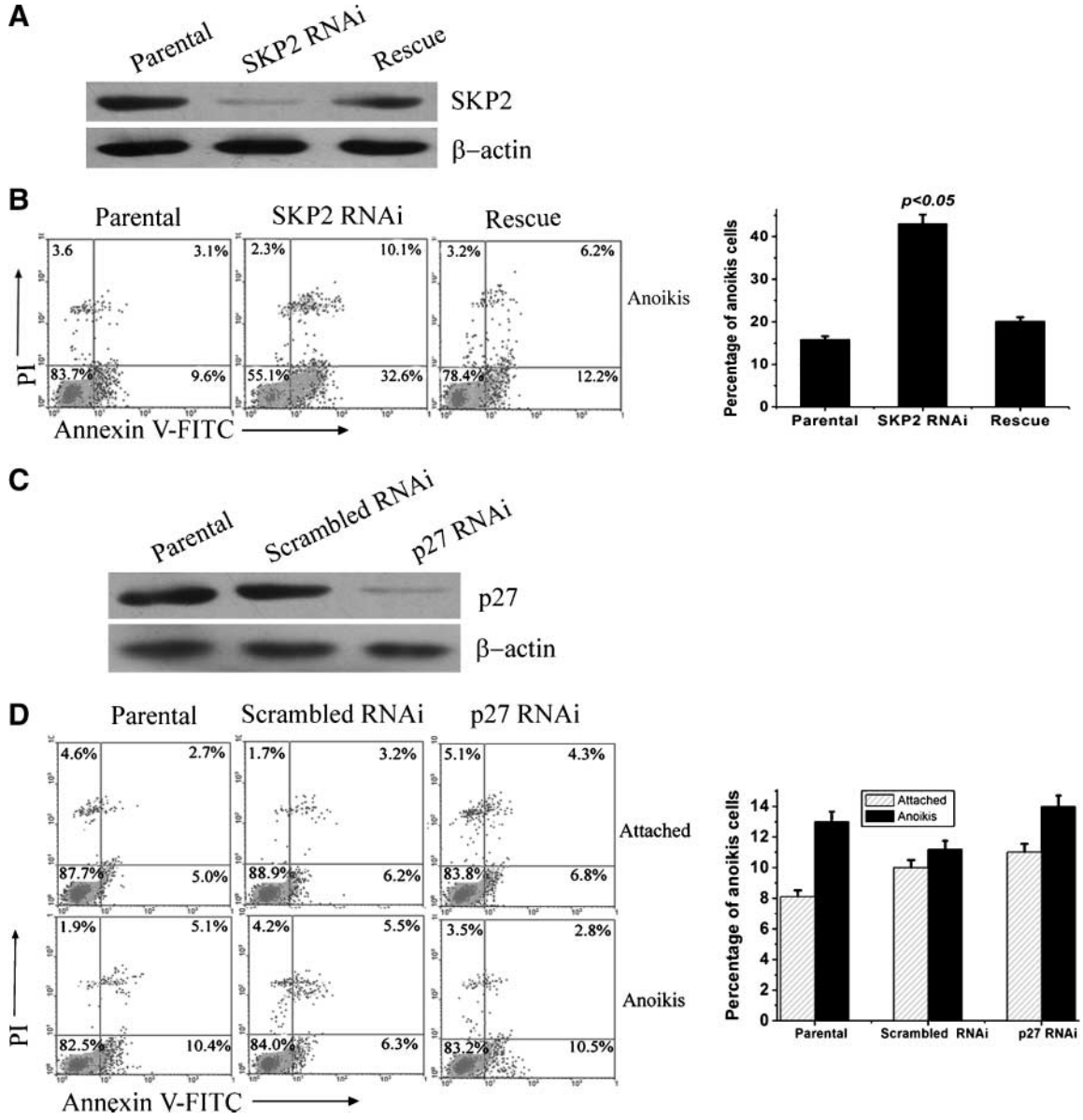


**FIGURE 5.** Rescue of the effects of SKP2 siRNA and the effects of p27 knockdown on anoikis in EC9706 cells. SKP2-shRNA–expressing EC9706 cells were transiently transfected with empty vector (data not shown) or with a SKP2 construct bearing a triple-point mutation in the 19-bp sequence that we selected as a target for the shRNA. This mutation does not affect the amino acid sequence of the protein. **A.** Expression levels of SKP2 in the parental, SKP2 RNAi, and rescue groups. **B.** Percentage of anoikis cells in the rescue group was significantly lower than that of the SKP2 RNAi group. **C.** Western blotting analysis of p27 expression in three groups. **D.** Anoikis cell percentages of parental, scrambled RNAi, and p27 RNAi groups in attached and detached conditions were not significantly different.

with parental EC9706 cells and two with scrambled RNAi cells, but none with SKP2 RNAi cells, developed visually observable lung nodules (Fig. 7C). SKP2 expression was validated in the formalin-fixed, paraffin-embedded sections of the subcutaneous tumors by immunohistochemical staining (Fig. 8A).

Because tumor growth is determined by the balance of cell proliferation and programmed cell death, cell proliferation–related protein Ki-67 was analyzed on subcutaneous tumor sections by immunohistochemistry. No difference was observed between these three groups of tumors. Expression of p27 increased in SKP2 RNAi group (Fig. 8A). Apoptosis in the subcutaneous tumor sections was examined by TUNEL assays: Few apoptotic cells were found in the tumors derived from scrambled RNAi and parental EC9706 cells. In contrast, significantly more apoptotic cells were detected in the tumors of SKP2 RNAi–treated mice ($P < 0.05$; Fig. 8B and C). These results indicated that SKP2 RNAi in esophageal cancer cells suppressed *in vivo* tumor growth by promoting apoptosis.

## Discussion

In the present work, we examined the genomic amplification and expression of SKP2 by FISH, reverse transcription-PCR, and Western blotting in ESCC tissues. Overexpression of SKP2

was found in the same tumors with *SKP2* gene amplification. In addition, the frequency of *SKP2* amplification by FISH (46%) in tumors was parallel to that of overexpression by immunohistochemical staining (51%). These findings suggest for the first time that DNA amplification is one of the mechanisms activating *SKP2* gene in ESCC. Further statistical analysis revealed that amplification and overexpression of SKP2 were significantly associated with positive lymph node metastasis and tumor stage. Immunohistochemical analyses by other investigators also revealed that overexpression of SKP2 was associated with lymph node metastasis in oral squamous cell carcinoma (19) and laryngeal squamous cell carcinoma (20). Significantly inverse correlation between SKP2 and p27 expression was found in ESCC, which was concordance with reports in other tumors (16, 17, 21). Moreover, the negative correlation was confirmed by Western blotting both in attached and detached EC9706 cells. This study has shown the first evidence that amplification and elevated expression of SKP2 were associated with indicators of malignancy in ESCC, such as positive lymph node metastasis and advanced stage. Metastasis to lymph nodes is a major obstacle for successful treatment of ESCC. Our results suggest that SKP2 may be a useful diagnostic biomarker for metastatic potential in ESCC.

Given that migration and invasion is an essential part of the metastatic process, we performed stable transfection in cultured EC9706 cells that have amplification and high expression of SKP2 to investigate the effect of the gene on migration and invasion. The transfection induced a decrease in SKP2 protein and consequent inhibition of invasion and migration of these cells. Transient transfection with a chemically synthesized siRNA was also done and the results were similar (data not shown). Yokoi et al. (15) have previously reported that down-regulation of SKP2 by antisense treatment induced apoptosis and inhibited invasion and migration in lung cancer cells. However, our results showed that SKP2 has no effect on apoptosis of attached cells.

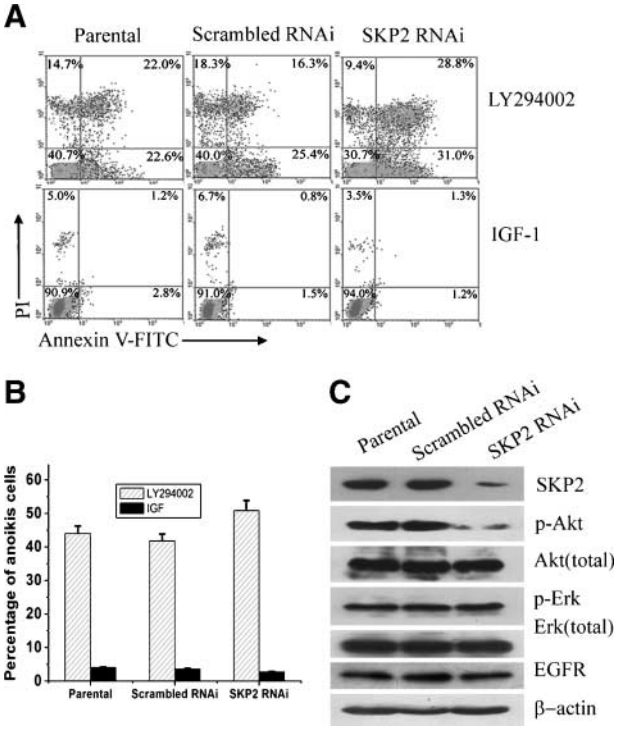


**FIGURE 6.** Silencing of SKP2 in EC9706 promoted anoikis via inactivation of the PI3K-Akt pathway. **A.** Representative images of flow cytometry analysis of apoptotic cells by Annexin V-FITC/propidium iodide staining. **B.** Flow cytometry results were plotted as mean from triplicate experiments; bars, SD. **C.** Down-regulation of SKP2 led to decreased activation of Akt, as evident from decreased levels of phosphor-Akt (Ser473). No changes in pErk or EGFR expression were observed.

Metastasis is a multistep process facilitated by the evolution of anoikis-resistant subsets of cancer cells that are capable of surviving in the bloodstream during dissemination after they detach from the primary tumor and its stroma. Anoikis, a Greek word meaning loss of ''home'' or ''homelessness,'' was originally defined by Frisch a decade ago as a unique phenomenon reflecting apoptotic cell death as a direct consequence of insufficient cell-matrix interaction (22, 23) and was later recognized as a potentially significant factor in tumor angiogenesis and metastasis (18, 24). As a functional phenomenon, anoikis can suppress expansion of oncogenically transformed cells by preventing proliferation at migrating locations, whereas migrating tumor cells that are resistant to anoikis induction can grow at inappropriate locations (25, 26). Resistance to anoikis is thus emerging as a hallmark of metastatic cancer cells, especially because anchorage-independent growth of tumor cells is a classic characteristic of different types of human malignancies. Expression of certain oncogenes can provide protection from anoikis. We have investigated whether SKP2 can protect cells from anoikis: Our findings suggested that decreased SKP2 expression in EC9706 cells by RNAi was associated with increased anoikis. This is the first report that SKP2 is involved in anoikis resistance. Given the report of Collins et al. (27) that overexpression of p27 conferred anoikis resistance in MCF-10A cells and p27 is one of the most important substrates for SKP2, we also detected the effect of p27 on anoikis. The results showed that knockdown of p27 had no effect on anoikis in EC9706 cells, suggesting the effect of SKP2 on anoikis in ESCC was not mediated by p27. The probable reasons that led to these different results were that (*a*) the cell line was different in these two experiments, and (*b*) SKP2 is amplified and overexpressed in ESCC and it is the upstream protein for p27, so the effect of SKP2 is dominant. Kim et al. (28) proposed that galectin-3 inhibition of anoikis involves cell cycle arrest at an anoikis-insensitive point (late $G_1$) through modulation of gene expression and activities of cell cycle regulators. Collins et al. (27) also reported that $G_1$-S cell cycle arrest provides anoikis resistance through Erk-mediated Bim suppression. However, our results showed that SKP2 knockdown had no effect on cell cycle progress of EC9706 cells during induction of anoikis on polyHEMA plates. Thus, other mechanisms may be involved in the anoikis induced by SKP2 knockdown.

Although the underlying mechanisms rendering anoikis resistance in cancer cells are not fully understood, several signal pathways have been described in different cell types, including the PI3K-Akt, MEK-Erk, and EGFR pathways (22, 23, 29). Our data showed that Akt phosphorylation decreased after SKP2 RNAi transfection, and no changes were observed in Erk phosphorylation and EGFR. Moreover, knockdown of SKP2

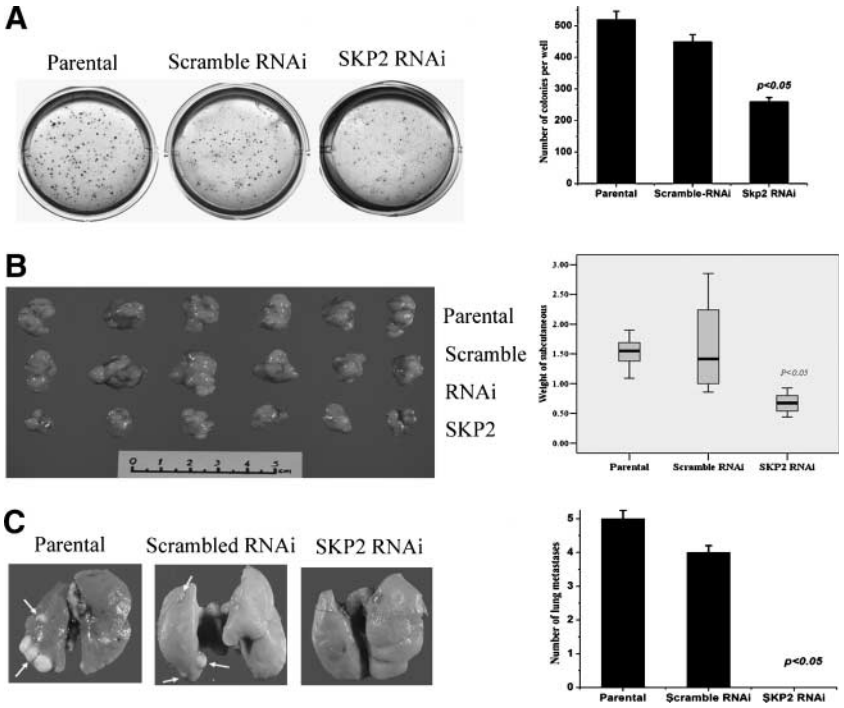


**FIGURE 7.** Effects of SKP2 RNAi on colony formation in soft agar and subcutaneous tumor growth in nude mice. **A.** Representative photos and statistical plot in soft agar assay. **B.** Tumors at 12 wk postinjection and statistical plot of tumor weights. **C.** Down-regulation of SKP2 in EC9706 dramatically reduced lung metastasis of tumors in nude mice.

had no more effects on anoikis after treatment of cells with PI3K-Akt pathway inhibitor or activator. Thus, PI3K-Akt, but not MEK-Erk or EGFR signaling, contributed to SKP2-related survival in detached cells. These results confirmed our hypothesis that the mechanism of anoikis resistance induced by SKP2 was not mediated by cell cycle arrest. However, when PI3K activity was inhibited by LY294002, SKP2 RNAi could still increase anoikis to some extent, suggesting that other pathways, in addition to PI3K, may participate in SKP2-related anoikis resistance.

Some studies about the relationship between PI3K/Akt pathway and SKP2 have been reported. Reichert et al. (30) showed that in pancreatic ductal adenocarcinoma cells, PI3K/Akt signaling was linked to *SKP2* gene transcription via control of a *cis*-acting element, E2F1, binding to the proximal human *SKP2* gene promoter. At the same time, the degradation of E2F1 in S-$G_2$ phase was mediated by $SCF^{SKP2}$ complex (31). Others have also reported that PI3K/Akt signaling controls SKP2 transcription in different cellular systems (32). However, whether SKP2 also can affect the PI3K-Akt pathway still remains unclear. Our data showed that overexpression of SKP2 in ESCC was the result of gene amplification, and decreased SKP2 by RNAi reduced pAkt expression, suggesting that SKP2 also has an effect on the PI3K/Akt pathway through an unknown mechanism. These results suggest a possible negative feedback loop between PI3K/Akt and SKP2 that may help to maintain the balance between cell survival and apoptosis. The mechanism of how SKP2 affects the PI3K/Akt pathway awaits further investigation.

Taken together, our data suggest that SKP2 is an oncogene in the 5p13 amplicon, which exerts functions on tumor metastasis in ESCC. Future studies will need to address whether targeted therapies directed against SKP2 will inhibit metastasis in ESCC.

## Materials and Methods

### *Tissue Specimens*

Fresh tissues containing ESCCs and adjacent histologically normal epithelia were procured from surgical resection specimens collected by the Department of Pathology in Cancer Hospital, Chinese Academy of Medical Sciences, Beijing, China. Primary tumor regions and the corresponding histologic normal esophageal mucosa from the same patients were separated by experienced pathologists and immediately stored at −70°C until use. All patients received no treatment before surgery and signed informed consent forms for sample collection. Use of patient samples of tumor and adjacent histologically normal tissues had been approved by our institutional ethics committee.

### *FISH*

Tumor tissues were scraped and then digested with 0.2% type II collagenase (Sigma). Cells were incubated in 0.075 mol/L KCl hypotonic buffer at 37°C for 60 min and fixed in methanol/acetic acid (3:1, v/v) at 4°C. Single-cell suspensions were dropped on cool wet slides. After air-drying overnight, slides were sequentially treated with RNase and pepsin. Denaturation was in 70% formamide, 2× SSC (pH 7) for 3 min at 75°C. BAC clones of SKP2 (RP11-816N21, Invitrogen) and 5q35 locus (RP11-51d11) were labeled by random primer technique with Cy3-dUTP and FITC-dUTP, respectively. The probe mixture was denatured at 74°C for 8 min and then hybridized to denatured slides at 37°C for 48 h. Posthybridization washes were carried out in 50% formamide for 15 min and twice in 2× SSC. Slides were counterstained with 4′,6-diamidino-2-phenylindole. Gray images were captured with a cooled charge-coupled device camera (Princeton, Inc.) equipped with an Opton fluorescence

microscope. The images were analyzed using the MetaMorph Imaging System (Universal Imaging Corp). Probes were tested by FISH on interphase nuclei and metaphase spreads from normal lymphocytes and yielded two signals. One hundred interphase cell nuclei of each tumor sample were analyzed and ratios (target BAC/control) of >2 were assessed as amplification (33).

### *DNA Extraction and Real-time PCR*

Tissues were digested with 50 mg/mL proteinase K in 1% SDS for 12 h at 48°C and extracted with phenol/chloroform. DNA was precipitated with cold ethanol and dissolved in water. Genomic copy number of SKP2 was evaluated by real-time PCR on an ABI Prism 7300 (Applied Biosystems) with SYBR Green PCR core reagents according to the manufacturer's protocol. GAPDH was applied as the input reference. The primers used for genomic SKP2 detection were 5′-AGCACCTCCAGGAGATTCCAGACCTGAGTAG-3′ (forward) and 3′-AGGTCTGCCATAGAGACTCATCA-GACGCTAGG-5′ (reverse). The mean SKP2 level of the three real-time quantitative PCR experiments was calculated for each case. Results of the real-time PCR data are presented as $C_T$ values, which is defined as the threshold PCR cycle number at which an amplified product is first detected. The average $C_T$ was calculated for both SKP2 and GAPDH, and $\Delta C_T$ was determined as the mean of the triplicate $C_T$ values for SKP2 minus the mean of the triplicate $C_T$ values for GAPDH. The $\Delta\Delta C_T$ represents the difference between the paired tissue samples, as calculated by the formula $\Delta\Delta C_T = (\Delta C_T \text{ of tumor} - \Delta C_T \text{ of normal})$. The relative copy number of SKP2 for a tumor sample compared with its normal epithelial counterpart was expressed as $2^{-\Delta\Delta C_T} \times 2$. Using this method, the data are presented as the fold change in the target gene (*SKP2*) in tumor normalized to an internal control gene (*GAPDH*) and relative to the nontumor control.

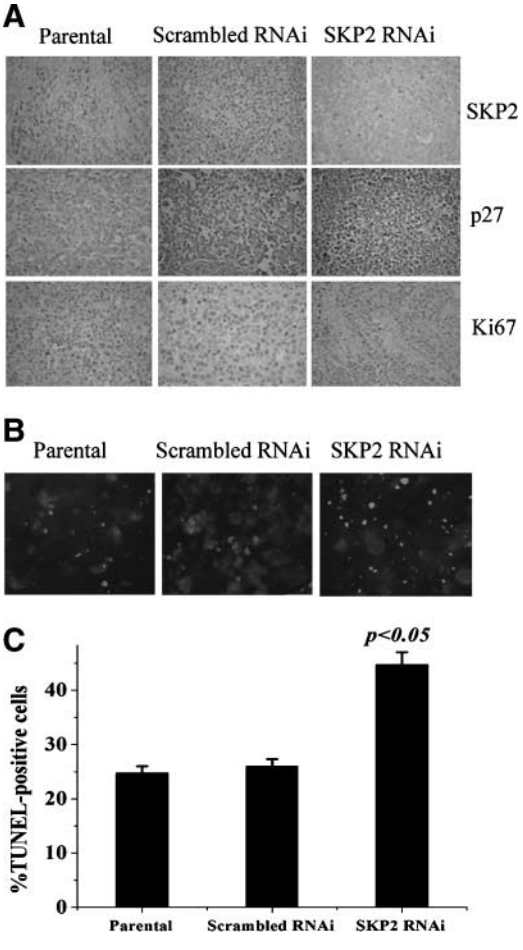


**FIGURE 8.** **A.** Formalin-fixed, paraffin-embedded sections of the subcutaneous tumors from parental EC9706, scrambled RNAi, and SKP2 RNAi cells were analyzed by immunohistochemical staining of SKP2 and p27. **B.** Subcutaneous tumor sections were analyzed by TUNEL assay. Total DNA was stained with 4′,6-diamidino-2-phenylindole and apoptotic cells were visualized by TUNEL. **C.** Percentage of TUNEL-positive cells in subcutaneous tumor sections. Columns, mean; bars, SD.

### *RNA Extraction and Reverse Transcription-PCR*

Total RNA was prepared using Trizol reagent (Life Technologies, Inc.) according to the manufacturer's instruction. Five micrograms of total RNA were used to synthesize the first strand of cDNA using SuperScript II RT 200 units/μL (Invitrogen). Primers designed for SKP2 were 5′-CTTTCTG-GGTGTTCTGGATT-3′ as forward and 5′-GGTGTTGGAGG-TAGTTGAGC-3′ as reverse. GAPDH was used to ascertain the equal amount of cDNA in each reaction. The PCR program was as follows: denaturation at 95°C for 4 min, 25 cycles of 95°C for 40 s, 58°C for 40 s, and 72°C for 50 s, followed by a 72°C elongation step for 6 min. Twenty microliters of each PCR product were resolved by 2% (w/v) agarose gel electrophoresis.

### *ESCC Tissue Microarray and Immunohistochemical Staining*

A total of 140 formalin-fixed, paraffin-embedded ESCCs and the corresponding normal epithelia were placed on the tissue microarray. For each case, normal tissues were repeated thrice and cancer tissues were repeated five times. For immunohistochemical analysis, the slides were deparaffinized, rehydrated, then immersed in 3% hydrogen peroxide solution for 10 min, heated in EDTA buffer (pH 8.0) at 95°C for 25 min, and cooled at room temperature for 60 min. The slides were blocked by 10% normal goat serum at 37°C for 30 min, and then incubated with rabbit polyclonal antibody against SKP2 (1:200, Santa Cruz), p27 (1:200, Santa Cruz), and Ki67 (1:200, Santa Cruz), respectively, overnight at 37°C. After washing with PBS, the slides were incubated with biotinylated second antibody (diluted 1:100) for 30 min at 37°C, followed by streptavidin-peroxidase (1:100 dilution) incubation at 37°C for 30 min. Immunolabeling was visualized with a mixture of 3,3′-diaminobenzidine solution. Counterstaining was carried out with hematoxylin.

Expression score of SKP2 was determined by staining intensity and immunoreactive cell percentage. The staining intensity was scored into three grades: 0 for complete absent staining, 1 for weak staining, and 2 for strong staining. The extent of positively stained nuclei was scored into three grades: 0 for <10%, 1 for 10% to 30%, and 2 for >30%. The final score

for each tumor sample represents the sum of staining intensity and extent (20, 34). The expression of p27 and Ki67 was graded as high (>30% of tumor cells showed strong or diffuse immunopositivity), moderate (5-30% of tumor cells showed moderate or patchy immunopositivity), or low (<5% of the tumor cells showed weak or focal immunopositivity or no staining; ref. 35).

### Plasmid Construction and SiRNA Synthesis

PSuppressorNeo expression vector was applied to generate biologically active siRNAs for sustained gene knockdown. The sequences of insert SKP2 and p27 siRNA were prepared by the synthesizing and annealing two complementary oligonucleotidesas, respectively: SKP2, 5′-tcgaGGGAGTGACAAAGACTTTGgagtactgCAAAGTCTTTGTCACTCCCTTTTT-3′ and 5′-ctagAAAAAGGGAGTGACAAAGACTTTGcagtactcCAAAGTCTTTGTCACTCCC-3′ (36); p27, 5′-gagtactgCCTCTCCTCTCCGCCCTCCgagtactgGGAGGGCGGAGAGGAGAGGTTTTT-3′ and 5′-ctgaAAAAACGCGCAGGGGCTGCGGGGcagtactcCCCCGCAGCCCCTGCGCG-3′. A scrambled sequence without significant homology to human gene sequences was used as a control. Mutant pcDNA3.1-SKP2, preserving the same amino acid sequence but containing three point mutations in the target nucleotide sequence and therefore resistant to SKP2-shRNA, was produced by GeneChem Company.

### Cell Culture and Transfection

The esophageal squamous cell carcinoma EC9706 cell line was established and previously studied in our laboratory (37). Cells were cultured in RPMI 1640 (Invitrogen) supplemented with 10% fetal bovine serum. Cell transfections were done using Lipofectamine 2000 (Invitrogen) according to the manufacturer's instruction. In transient transfection, 100 nmol/L of SKP2 siRNA or scrambled siRNA were used and cells were harvested 48 h after transfection. In the stable transfection, cells were selected with 200 μg/mL G418 and clones were isolated by serial dilution. The pool of SKP2 RNAi and p27 RNAi clones was chosen for subsequent experiments.

### Western Blot Analysis

Whole cell extracts were prepared from ESCC tissues and cultured cells by homogenizing cells in a lysis buffer [10 mmol/L Tris-HCl (pH 7.5), 150 mmol/L NaCl, 1% NP40] containing a cocktail of protease inhibitors. After centrifugation at 15,000 RCF for 30 min at 4°C, supernatants were recovered and used for immunoblot analysis. The proteins were separated by SDS-PAGE and then transferred onto polyvinylidene difluoride membranes (Millipore). Blots were blocked and then probed with antibodies against SKP2 (1:500 dilution; Santa Cruz), p27 (1:500 dilution; Santa Cruz), p21 (1:500 dilution; Santa Cruz), β-actin (1:5,000 dilution; Sigma), Akt (1:1,000 dilution; Santa Cruz), pAkt (Ser473, 1:400 dilution; Santa Cruz), Erk (1:1,000 dilution; Santa Cruz), pErk (Tyr204, 1:400 dilution; Santa Cruz), EGFR (1:500 dilution; Santa Cruz), caspase-3 (1:500 dilution; Santa Cruz), and PARP (1:500 dilution; CST). After washing, the blots were incubated with horseradish peroxidase–conjugated secondary antibodies and visualized by super ECL detection reagent (Applygen).

### Migration and Invasion Assays

For haptotactic cell migration assay, $1 \times 10^5$ SKP2 RNAi, scrambled RNAi, and parental EC9706 cells were seeded on a fibronectin-coated polycarbonate membrane insert (6.5 mm in diameter with 8.0-μm pores) in a transwell apparatus (Costar) and cultured in RPMI 1640. Fetal bovine serum was added to the lower chamber. After incubation for 12 h at 37°C in a $CO_2$ incubator, the insert was washed with PBS and cells on the top surface of the insert were removed by wiping with a cotton swab. For the Matrigel chemoinvasion assay, the procedure was similar with the haptotactic cell migration assay, except that the transwell membrane was coated with 300 ng/μL Matrigel (BD Biosciences) and the cells were incubated for 24 h at 37°C. Cells that migrated to the bottom surface of the insert were fixed with methanol and stained by 0.4% crystal violet and then subjected to microscopic inspection. Cells were counted based on five field digital images taken randomly at ×200.

### Assessment of Anoikis, Cell Cycle, and Inhibitor Treatment

Cells were prevented from adhering to the plastic dishes by culturing them in dishes coated with PolyHEMA (Sigma) as described previously (22). After 24-h growth in suspension, cells were harvested for apoptosis measurement with Annexin V-FITC apoptosis detection kit (Sigma) and cell cycle detection with propidium iodide staining and subsequently analyzed by flow cytometry. PI3K inhibitor LY294002 (2-(4-morpholinyl)-8-phenyl-4*H*-1-benzopyran-4-one; 10 μmol/L; Calbiochem) and 10 ng/mL activator insulin-like growth factor I (ProspecTany TechnoGene) were used in the anoikis assay.

### Soft Agar Assay and Tumor Formation in Nude Mice

Soft agar assays were done as described (23). SKP2 RNAi, scrambled RNAi, and parental EC9706 cells were plated in six-well plates at a density of 500 per well. After 3 wk of incubation at 37°C, 5% $CO_2$, colonies were stained with 0.2% *p*-iodonitrotetrazolium violet and counted. To assay tumor formation in nude mice, cloned pools of SKP2 transfectants, scrambled RNAi, and parental EC9706 were trypsinized, counted, and resuspended in 1× PBS. One hundred microliters of 1× PBS containing $10^6$ cells were then infected into 4- to 5-wk-old female nude mice. The mice were sacrificed 12 wk after injection and examined for subcutaneous tumor growth and metastasis development. To clearly observe the metastasis nodules in the lung, we fixed the lung in Bouin's solution and counted the visually observable metastases.

### TUNEL Assay

The formalin-fixed, paraffin-embedded sections of subcutaneous tumors from nude mice were analyzed by using the DeadEnd Fluorometric TUNEL System (Promega). The assay was done according to the user manual. Total DNA was stained with 4′,6-diamidino-2-phenylindole, and apoptotic cells appeared in green color with the FITC filter under a fluorescent microscope.

*Statistical Analysis*

All statistical analyses were done using SPSS13.0 software. We statistically evaluated experimental results using the Kruskal-Wallis test, Mann-Whitney test, and ANOVA test. $P < 0.05$ was considered statistically significant.

## Disclosure of Potential Conflicts of Interest

No potential conflicts of interest were disclosed.

## References


1. Bockmuhl U, Petersen S, Schmidt S, et al. Patterns of chromosomal alterations in metastasizing and nonmetastasizing primary head and neck carcinomas. Cancer Res 1997;57:5213–6.

2. Wei F, Ni J, Wu SS, et al. Cytogenetic studies of esophageal squamous cell carcinomas in the northern Chinese population by comparative genomic hybridization. Cancer Genet Cytogenet 2002;138:38–43.

3. Balsara BR, Testa JR. Chromosomal imbalances in human lung cancer. Oncogene 2002;21:6877–83.

4. Bjorkqvist AM, Husgafvel-Pursiainen K, Anttila S, et al. DNA gains in 3q occur frequently in squamous cell carcinoma of the lung, but not in adenocarcinoma. Genes Chromosomes Cancer 1998;22:79–82.

5. Zhang H, Kobayashi R, Galaktionov K, Beach D. p19Skp1 and p45Skp2 are essential elements of the cyclin A-CDK2 S phase kinase. Cell 1995;82:915–25.

6. Demetrick DJ, Zhang H, Beach DH. Chromosomal mapping of the genes for the human CDK2/cyclin A-associated proteins p19 (SKP1A and SKP1B) and p45 (SKP2). Cytogenet Cell Genet 1996;73:104–7.

7. Nakayama K, Nagahama H, Minamishima YA, et al. Targeted disruption of Skp2 results in accumulation of cyclin E and p27(Kip1), polyploidy and centrosome overduplication. EMBO J 2000;19:2069–81.

8. Bhattacharya S, Garriga J, Calbo J, Yong T, Haines DS, Grana X. SKP2 associates with p130 and accelerates p130 ubiquitylation and degradation in human cells. Oncogene 2003;22:2443–51.

9. Tedesco D, Lukas J, Reed SI. The pRb-related protein p130 is regulated by phosphorylation-dependent proteolysis via the protein-ubiquitin ligase SCF(Skp2). Genes Dev 2002;16:2946–57.

10. Kamura T, Hara T, Kotoshiba S, et al. Degradation of p57Kip2 mediated by SCFSkp2-dependent ubiquitylation. Proc Natl Acad Sci U S A 2003;100:10231–6.

11. Bornstein G, Bloom J, Sitry-Shevah D, Nakayama K, Pagano M, Hershko A. Role of the SCFSkp2 ubiquitin ligase in the degradation of p21Cip1 in S phase. J Biol Chem 2003;278:25752–7.

12. von der Lehr N, Johansson S, Wu S, et al. The F-box protein Skp2 participates in c-Myc proteosomal degradation and acts as a cofactor for c-Myc-regulated transcription. Mol Cell 2003;11:1189–200.

13. Kim SY, Herbst A, Tworkowski KA, Salghetti SE, Tansey WP. Skp2 regulates Myc protein stability and activity. Mol Cell 2003;11:1177–88.

14. Masuda TA, Inoue H, Sonoda H, et al. Clinical and biological significance of S-phase kinase-associated protein 2 (Skp2) gene expression in gastric carcinoma: modulation of malignant phenotype by Skp2 overexpression, possibly via p27 proteolysis. Cancer Res 2002;62:3819–25.

15. Yokoi S, Yasui K, Saito-Ohara F, et al. A novel target gene, SKP2, within the 5p13 amplicon that is frequently detected in small cell lung cancers. Am J Pathol 2002;161:207–16.

16. Gstaiger M, Jordan R, Lim M, et al. Skp2 is oncogenic and overexpressed in human cancers. Proc Natl Acad Sci U S A 2001;98:5043–8.

17. Fukuchi M, Masuda N, Nakajima M, et al. Inverse correlation between expression levels of p27 and the ubiquitin ligase subunit Skp2 in early esophageal squamous cell carcinoma. Anticancer Res 2004;24:777–83.

18. Christofori G. Changing neighbours, changing behaviour: cell adhesion molecule-mediated signalling during tumour progression. EMBO J 2003;22:2318–23.

19. Shintani S, Li C, Mihara M, Hino S, Nakashiro K, Hamakawa H. Skp2 and Jab1 expression are associated with inverse expression of p27(KIP1) and poor prognosis in oral squamous cell carcinomas. Oncology 2003;65:355–62.

20. Dong Y, Sui L, Watanabe Y, Sugimoto K, Tokuda M. S-phase kinase-associated protein 2 expression in laryngeal squamous cell carcinomas and its prognostic implications. Oncol Rep 2003;10:321–5.

21. Kudo Y, Kitajima S, Sato S, Miyauchi M, Ogawa I, Takata T. High expression of S-phase kinase-interacting protein 2, human F-box protein, correlates with poor prognosis in oral squamous cell carcinomas. Cancer Res 2001;61:7044–7.

22. Frisch SM, Francis H. Disruption of epithelial cell-matrix interactions induces apoptosis. J Cell Biol 1994;124:619–26.

23. Frisch SM, Screaton RA. Anoikis mechanisms. Curr Opin Cell Biol 2001;13:555–62.

24. Hanahan D, Weinberg RA. The hallmarks of cancer. Cell 2000;100:57–70.

25. Bourguignon LY, Zhu H, Shao L, Chen YW. CD44 interaction with c-Src kinase promotes cortactin-mediated cytoskeleton function and hyaluronic acid-dependent ovarian tumor cell migration. J Biol Chem 2001;276:7327–36.

26. Ramachandra M, Atencio I, Rahman A, et al. Restoration of transforming growth factor β signaling by functional expression of smad4 induces anoikis. Cancer Res 2002;62:6045–51.

27. Collins NL, Reginato MJ, Paulus JK, et al. $G_1$/S cell cycle arrest provides anoikis resistance through Erk-mediated Bim suppression. Mol Cell Biol 2005;25:5282–91.

28. Kim HR, Lin HM, Biliran H, Raz A. Cell cycle arrest and inhibition of anoikis by galectin-3 in human breast epithelial cells. Cancer Res 1999;59:4148–54.

29. Reginato MJ, Mills KR, Paulus JK, et al. Integrins and EGFR coordinately regulate the pro-apoptotic protein Bim to prevent anoikis. Nat Cell Biol 2003;5:733–40.

30. Reichert M, Saur D, Hamacher R, Schmid RM, Schneider G. Phosphoinositide-3-kinase signaling controls S-phase kinase-associated protein 2 transcription via E2F1 in pancreatic ductal adenocarcinoma cells. Cancer Res 2007;67:4149–56.

31. Nakayama KI, Nakayama K. Ubiquitin ligases: cell-cycle control and cancer. Nat Rev Cancer 2006;6:369–81.

32. Andreu EJ, Lledo E, Poch E, et al. BCR-ABL induces the expression of Skp2 through the PI3K pathway to promote p27Kip1 degradation and proliferation of chronic myelogenous leukemia cells. Cancer Res 2005;65:3264–72.

33. Sen S, Zhou H, Zhang RD, et al. Amplification/overexpression of a mitotic kinase gene in human bladder cancer. J Natl Cancer Inst 2002;94:1320–9.

34. Zhu CQ, Blackhall FH, Pintilie M, et al. Skp2 gene copy number aberrations are common in non-small cell lung carcinoma, and its over-expression in tumors with ras mutation is a poor prognostic marker. Clin Cancer Res 2004;10:1984–91.

35. Kudo Y, Takata T, Yasui W, et al. Reduced expression of cyclin-dependent kinase inhibitor p27Kip1 is an indicator of malignant behavior in oral squamous cell carcinoma. Cancer 1998;83:2447–55.

36. Kudo Y, Kitajima S, Ogawa I, Kitagawa M, Miyauchi M, Takata T. Small interfering RNA targeting of S phase kinase-interacting protein 2 inhibits cell growth of oral cancer cells by inhibiting p27 degradation. Mol Cancer Ther 2005;4:471–6.

37. Han Y, Wei F, Xu X, et al. Establishment and comparative genomic hybridization analysis of human esophageal carcinomas cell line EC9706. Zhonghua Yi Xue Yi Chuan Xue Za Zhi 2002;19:455–7.